# Dynamic probing of plasma-catalytic surface processes: Oxidation of toluene on CeO2

Zixian Jia, Xianjie Wang, Frederic Thevenet, Antoine Rousseau

# Dynamic probing of plasma-catalytic surface processes: oxidation of toluene on $CeO_2$

Zixian JIA[1]*, Xianjie WANG[1], Frederic THEVENET[2,3], Antoine ROUSSEAU[1]*

[1] LPP, Ecole Polytechnique, UPMC, CNRS, Université Paris-Sud 11, 91128 Palaiseau Cedex, France

[2] Mines Douai, SAGE, F-59508 Douai, France

[3] Université de Lille, F-59000 Lille, France

Corresponding authors. E-mail: zixian.jia@lpp.polytechnique.fr and antoine.rousseau@lpp.polytechnique.fr

**Abstract**

This article reports the use of innovative diagnostics to monitor toluene adsorption and oxidation on $CeO_2$ surface under Non-Thermal Plasma (NTP) exposure. Two plasma-catalytic configurations are explored, namely: Post-Plasma Catalysis (PPC) and In-Plasma Catalysis (IPC). Since heterogeneous processes are pointed out as key steps of the plasma-catalyst coupling, the catalyst surface has been monitored by two complementary *in-situ* diagnostics: i) Diffuse Reflectance Infrared Fourier Transform Spectroscopy (DRIFTS) ii) and Transmission Fourier Transform Infrared Spectroscopy using Sorbent track (ST) device. Dielectric Barrier Discharges (DBD) are used in both PPC and IPC configurations to induce adsorbed toluene oxidation. Toluene in dry air is first adsorbed on the selected catalytic surface: ceria ($CeO_2$). Subsequently, the plasma is switched on. During the experiment, the ceria surface is monitored by infrared to study toluene adsorption and oxidation mechanisms. The adsorption capacity of toluene on ceria is respectively measured in the configurations of PPC and IPC by DRIFTS and ST. The oxidation of toluene by plasma follows a first-order reaction regardless of plasma configuration and injected power and IPC is more effective for the toluene removal than PPC. Intermediates of toluene (benzyl alcohol, benzaldehyde and benzoic acid) are also identified on the surface and their respective temporal evolutions as a function of the plasma exposure are studied.

**Keywords**

Plasma-catalysis, Adsorption, VOC, Non-Thermal Plasma, Air Treatment, Ceria, Toluene, DRIFTS

# 1 Introduction

Volatile organic compounds (VOCs) are organic chemical species characterized by high vapor pressures at room temperature, allowing their evaporation in air without decomposition. Atmospheric VOCs result from both biogenic and anthropogenic sources. VOC emissions can affect environment and human health in many ways [1], depending on various factors such as the structure of the VOCs, and the exposure parameters. Toluene is one of the most ubiquitous anthropogenic VOCs [2]. Due to its neurotoxic effects [3] several techniques have been studied in order to remove toluene such as photocatalysis [4], adsorption [5], bio-filtration [6], plasma-catalysis [7].

Among these methods, non-thermal plasma (NTP) is one of the most attractive due to its energy efficiency [8]. Regarding non-thermal plasma, the injected energy is used to generate energetic electrons while the background gas temperature remains close to ambient temperature. The collisions between the high-energy electrons and the background gas generate chemically active species (ions, radicals, excited species, etc) which directly or indirectly react with VOCs and induce oxidation reactions. In order to make reactions more selective and to prevent the formation of undesired by-products, the combination of plasma with heterogeneous catalysis has been addressed [9]. The catalysts can be placed downstream the plasma reactor, so-called Post Plasma Catalysis (PPC) [10,11], or directly introduced into the active plasma discharge, so-called In-Plasma Catalysis (IPC) [12,13]. Irrespectively of the configurations, synergetic effects involving catalytic surface reactions are observed [14,15]. Former studies pointed out various hypotheses to interpret plasma-catalyst positive interaction, among them ozone formation and decomposition [16], adsorption and desorption of organic reactants and plasma generated species [17], local heating [18], and enhanced interaction of gas-phase radicals with adsorbed pollutants [19]. These hypotheses are generally based on the monitoring of reactor outlet gases whereas they all refer to inner reactor processes. This

discrepancy motivates the development of *in-situ* diagnostics to deepen our understanding plasma-catalysis.

*In-situ* Fourier Transform Infrared (FTIR) spectroscopy allows real time monitoring of processes occurring on the surface of the catalysts. Diffuse Reflectance Infrared Fourier Transform Spectroscopy (DRIFTS) has been used by various authors to investigate adsorbed species and active site evolutions onto catalytic surfaces [20–22]. More precisely, in the case of PPC studies [23,24], Barakat et al. [24] investigated the evolution of adsorbed organics along the plasma-catalytic decomposition of acetone and isopropanol on $TiO_2$ surface using DRIFTS. Authors evidenced that complete oxidation of isopropanol and acetone is mainly limited by acetone oxidation rate. More recently, Magureanu et al. [25] used DRIFTS to address ozone interaction with Ag–Al catalysts supported on quartz pellets. This approach provided new insights into the determination of active sites for heterogeneous toluene mineralization. Regarding IPC, infrared (IR) absorption spectroscopy in transmission mode can be adapted to directly access the catalysts surface under plasma exposure. Noticeably, Rivallan et al. [26] achieved IR *in-situ* measurements combining a Dielectric-barrier discharge (DBD) with $Al_2O_3$ catalyst. Authors performed surface *in-situ* and time resolved monitoring of the oxidation of preliminarily adsorbed IPA. Another effective example can be found in the work of Stere et al. [27] who used DRIFTS to study the selective catalytic reduction (SCR) of NOx on a $Ag/Al_2O_3$ catalyst in the presence of toluene and n-octane where the catalyst was activated by a helium plasma jet at atmospheric pressure. The approaches of *in-situ* IR provide new insights into the catalyst surface during the pollutant adsorption and plasma induced oxidation process. Coupling this technique with *in-situ* plasma allowed real-time monitoring of (i) primary pollutants adsorption on the surface of the catalyst and (ii) the production of intermediates.

Our group recently reported a new approach to monitor adsorption and surface oxidation of pollutants under direct plasma exposure [28]. To that end, a new experimental device was

constructed and named Sorbent Track (ST). More precisely, the DBD is generated in contact with a catalytic pellet and transmission-FTIR measurements are performed throughout the plasma exposed pellet. Coupling this technique with *in-situ* plasma allowed real-time monitoring of species adsorbed, produced and removed from the catalyst surface. The sorbent-TRACK system made in our laboratory provides a quantitative insight to the heterogeneous processes of plasma catalysis [28].

In the present paper, adsorption and oxidation of toluene on ceria is reported under plasma exposure in two different configurations using surface monitoring diagnostics: In-Plasma Configuration (IPC) is studied using Sorbent TRACK; Post-Plasma Configuration (PPC) is studied using DRIFTS. With these two configurations, toluene was adsorbed up to its breakthrough onto $CeO_2$. Reversibly and irreversibly adsorbed toluene fractions are quantified and compared for IPC and PPC. The influence of plasma position and injected power are also investigated during the plasma oxidation process to know which configuration is more effective for toluene removal. Real time evolution of adsorbed intermediates of toluene is also reported.

# 2 Experimental set up

## 2.1 Gas flow preparation and materials

Toluene used in this study is provided by sigma Aldrich (34866, CHROMASOLV®, for HPLC, 99.9%). A 5.7 ml/min air flow were sent through the way (1) connected with the toluene bubbler of 273.15 K and the obtained toluene concentration at the bubbler outlet is 8964 ppm. A 494.3 ml/min air flow was sent through the way (2). Once the two ways were mixed together the concentration of toluene is 100 ppm with a flow rate of 500 mL $min^{-1}$. The material used as catalyst consists in $CeO_2$ powder (99.95% trace rare earth metals basis, sigma

Aldrich) with a specific surface area of 84 ± 5 $m^2/g$ measured by Brunauer-Emmett-Teller (BET) method (Coulter SA3100). In the DRIFTS experiments, 25.0 mg of $CeO_2$ powder are introduced into the sample holder. In the case of Sorbent Track experiments, $CeO_2$ powder has been compacted to a wafer (25.0 mg of $CeO_2$, Ø = 7 mm, thickness of 0.3 mm).

The experimental procedure is composed of four steps: i) thermal treatment of the catalyst at 400°C to remove water and other adsorbed hydrocarbon species; ii) adsorption of 100 ppm toluene onto the catalyst until saturation of the sorption sites; iii) flushing with dry air flow to remove reversibly adsorbed toluene; iv) surface exposition to *in-situ* plasma or *post-situ* plasma for two hours.

## *2.2 Post-Plasma (PPC) and In-Plasma (IPC) set-up*

The post situ plasma set-up is described in Figure 1a. For the *post-situ* plasma experiment, the DBD is placed upstream the catalyst bed. It consists of Pyrex glass tube of 23.5 cm length, 3.3 mm external diameter and 1.7 mm inner diameter. The high voltage electrode is a tungsten wire of 0.2 mm thickness placed in the middle of the tube. The ground electrode consists in a copper sheet wrapped around the dielectric Pyrex tube. The sample holder of DRIFTS consists in a ceramic crucible in which a few milligrams (ca. 25.0 mg) of the solid to be studied are placed. The cell contains a thermocouple and a heating resistor, a gas inlet and outlet, and ZnSe windows to allow the IR beam to enter and exit the cell. The infrared beam is focused by series of mirrors and the radiation diffused by the powder is collected by ellipsoidal mirrors and sent to the detector. The distance between the tail of plasma and the sample is 180 cm and the flow time of the active species before anchoring the catalyst is about 6 s. The detection and quantification of the gas phase species is performed using high resolution Nicolet 6700 Fourier Transform Infrared spectrometer (FTIR) equipped with a 10 m optical-path White cell and a cooled MCT (mercury cadmium telluride) detector.

The *in-situ* plasma set-up is described in Figure 1a. Sorbent Track cell is composed of a glass cylinder carrying a toroidal sample holder in its center where the ceria pellet is placed in the form of a self-supported wafer. The heating system gives a maximum temperature of 573 K on the sample. The plasma reactor consists of a Pyrex glass tube of 5.8 mm inner diameter, 8 mm outside diameter. The inner electrode (H.V.) consists of a copper wire of 30 µm and the outer electrode is a copper wire of 30 µm placed in the center of sample holder. More details of ST cell can be found in our previous study [28].

100 ppm of toluene diluted in air are sent into the DRIFTS or ST cell to saturated ceria surface. For PPC, the ceria surface is monitored by Diffuse Reflectance Infrared Fourier Transform Spectroscopy (DRIFTS) and the gas phase is measured using Fourier Transform Infrared Spectroscopy (FTIR). For IPC, the ceria surface is monitored by transmission FTIR. Figure 1c represents the absorbance spectra obtained by DRIFTS and ST when the ceria surface is saturated by toluene. The bands at 3030, 3054 and 3082 $cm^{-1}$ are assigned to toluene C–H aromatic and the C–H stretching from the toluene methyl group are detected at 2950, 2924 and 2879 $cm^{-1}$. The bands at 1495, 1460, 1562 and 1601 $cm^{-1}$ are attributed to the C=C stretching in the toluene aromatic ring. A small contribution at 1081 and 1032 $cm^{-1}$ could be attributed to in-plane toluene C–H bending. The intense band at 1297 $cm^{-1}$ might be assigned to toluene Ar-C stretching or to the twisting mode of methylene as proposed by Busca et al.[29]. Finally, a weak overtone in the 2000–1800 $cm^{-1}$ region is detected.

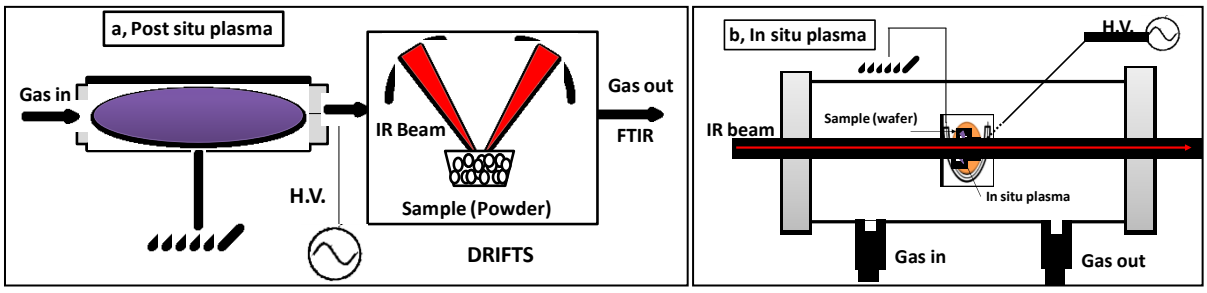

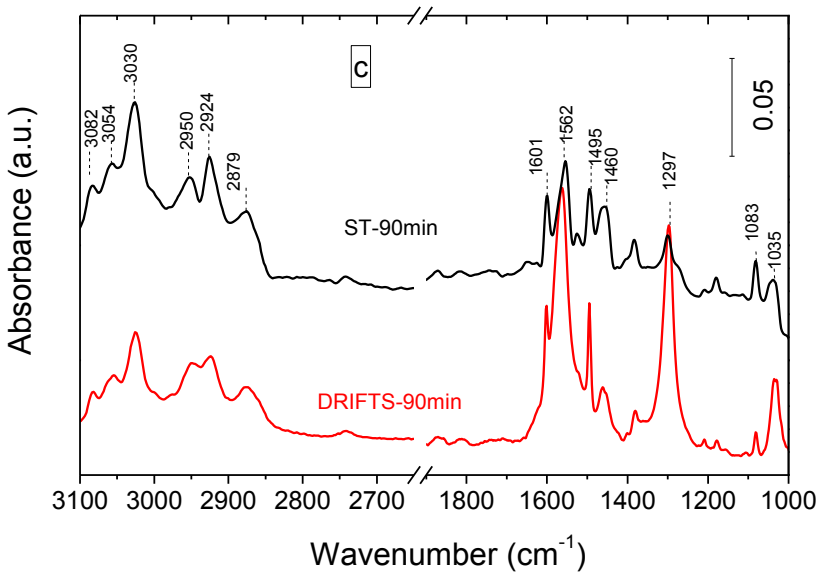


**Figure 1 - Schematic representation of experimental setups of PPC (a) and of IPC (b) and infrared absorbance spectra (c) of toluene adsorbed on ceria surface obtained by DRIFTS (red line) and ST (black line).**

## *2.3 Toluene quantification and intermediates identification*

Figure 2 represents the FTIR spectra of toluene and potential intermediates of toluene oxidation: benzoic acid, nitrobenzene, benzaldehyde and benzyl alcohol. In order to avoid overlapping, the bands of 2879 $cm^{-1}$ (ν(C-H) of toluene), 1754 $cm^{-1}$ (ν(C=O) of benzoic acid), 1715 $cm^{-1}$ (ν(C=O) of benzaldehyde), 1520 $cm^{-1}$ (ν(N=O) of nitrobenzene) and 1016 $cm^{-1}$ (ν(C-O) of benzyl alcohol) are respectively chosen to monitor the respective evolution of these adsorbed intermediates on ceria surface.

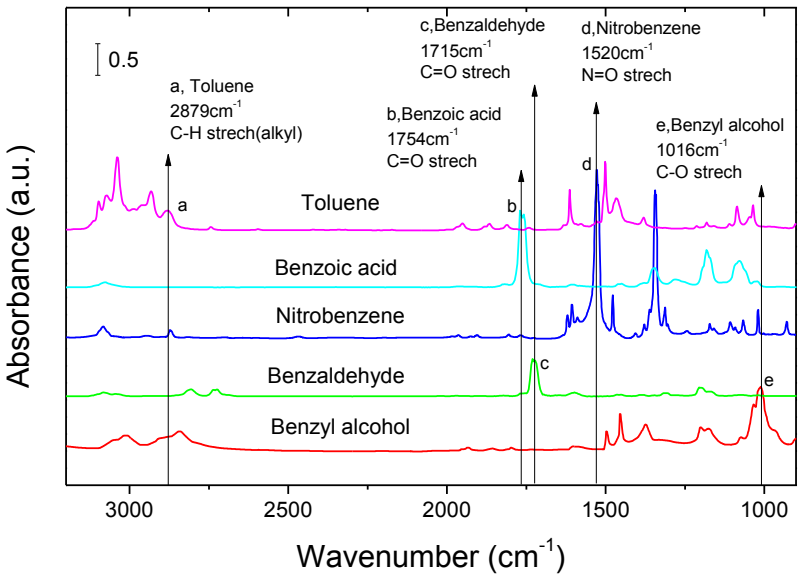


**Figure 2 - FTIR spectra of toluene (a), benzoic acid (b), nitrobenzene (c), benzaldehyde (d) and benzyl alcohol (e). Bands of 2879 $cm^{-1}$ (ν(C-H) of toluene), 1754 $cm^{-1}$ (ν(C=O) of benzoic acid), 1715 $cm^{-1}$ (ν(C=O) of benzaldehyde), 1520 $cm^{-1}$ (ν(N=O) of nitrobenzene) and 1016 $cm^{-1}$ (ν(C-O) of benzyl alcohol) are respectively chosen.**

For toluene, calibration curves (Figure 3) were obtained by passing the standard gases in air at different known concentrations (155, 100, 43, 21, 11 and 2ppm), through the 10 m white gas cell (black line in Figure 3a) or ST system (red line in Figure 3a). The fitting function is shown in Figure 3a, where the unit ppm was converted to $mol/cm^{-3}$. The spectral region selected for toluene (ν(C-H)) calibration is 2895.3-2871.1 $cm^{-1}$.

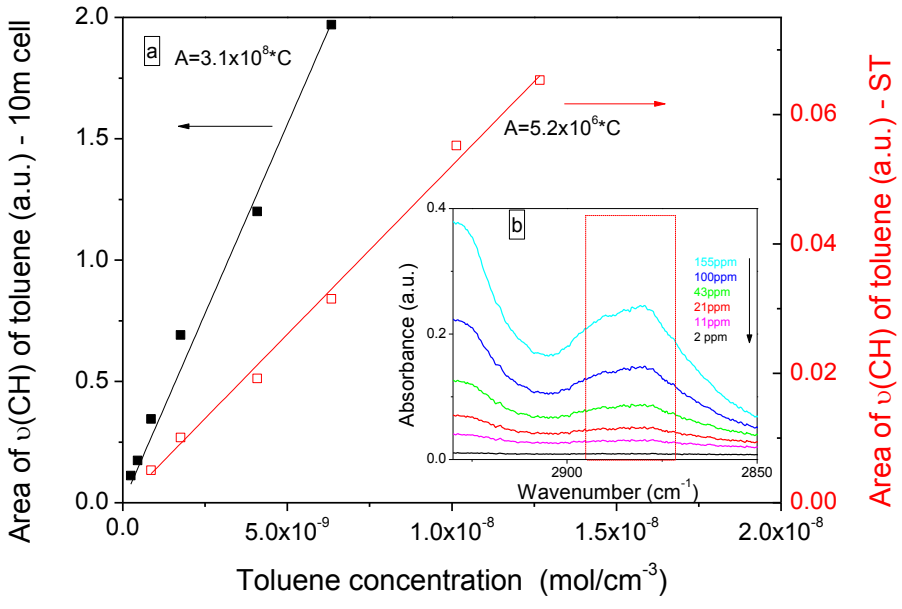

**Figure 3 - a) Corresponding toluene calibration curve (the spectral region of v(C-H) selected for toluene calibration is 2895.3-2871.1 $cm^{-1}$); b) Toluene FTIR spectra in the gas phase obtained in a 10 m White cell or ST with inlet toluene at a concentration of 155, 100, 43, 21, 11 and 2ppm in dry air (the unit ppm was converted to $mol/cm^{-3}$.).**

According to Lambert- Beer Law,

$$A_{toluene} = \varepsilon_{toluene} \cdot L \cdot C_{toluene} \quad \textbf{Equation 1}$$

For 10 m white gas cell, according to the slope of $3.1x10^8$ obtained in Figure 3b,

$$A_{toluene} = 3.1x10^5 \sigma_{toluene} \quad \textbf{Equation 2}$$

Where $\sigma_{toluene}$ are the LxC product expressed in $mol.cm^{-2}$

For Sorbent-TRACK system, L is 16 cm and with the slope of of $5.2x10^6$obtained in Figure 3b,

$$A_{toluene} = 3.2x10^5 \sigma_{toluene} \quad \textbf{Equation 3}$$

## *2.4 Electrical parameters measurement*

For both configurations, the electrical parameters were measured via two high voltage probes (LeCroy, PPE20KV-CC) connected to a digital oscilloscope (LeCroy WaveSurfer 64Xs-A, 600 MHz). A measurement capacitance (Cm) of 680 pF is placed in serie with the DBD reactors. The injected power is obtained from the Lissajous figures, corresponding to the plotting of the transported electric charges through the discharge as a function of the periodical applied voltage. Experimentally, charges are delivered from the voltage drop across the reactor and the average electric energy dissipated in a discharge cycle is proportional to the area of the characteristic Lissajous figure (Figure 4). In order to tune the specific input energy (SIE), the voltage applied is varied, but the frequency is kept constant at 50 Hz.

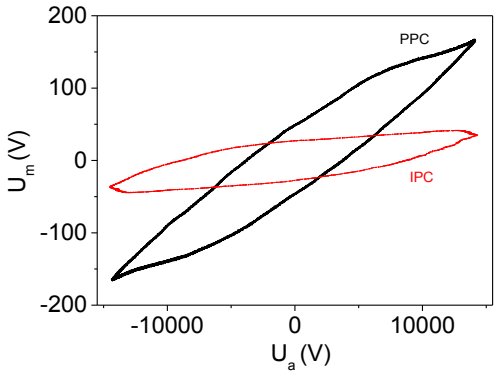


**Figure 4 - Example of Lissajous figure obtained from IPC (red) and PPC (black) to calculate injected powers. It is obtained by applying a voltage of 15 kV and a frequency of 50 Hz in a typical DBD reactor under air flow (500ml/min) by means of a sinusoidal power supply. Injected powers are respectively 130 and 145 mW for IPC and PPC.**

# 3 Results and discussions

## 3.1 Toluene adsorption and desorption

The toluene adsorption on ceria has been studied using two experimental set-ups: PPC and IPC. The purpose is to follow the evolution of toluene adsorption onto ceria, to determine the toluene adsorption capacity and to compare PPC and IPC approaches.

***Post-Plasma (PPC) set-up***

In order to saturate $CeO_2$ surface with the selected model VOC, 100 ppm of toluene diluted in air are sent into the cell (DRIFTS), with a total flow rate of 500 mL/min : gas phase measurements using FTIR and adsorbed phase measurements using DRIFTS. In order to determine ceria surface coverage by toluene, the adsorption capacity is determined from the FTIR measurements by the previously reported method [24]. Quantitative values of irreversibly and reversibly adsorbed toluene on ceria are determined using breakthrough curves as shown in Figure 5 in a dedicated experimental set up [24]. The mixig curve of the system is determined by sending the VOC in the empty reactor and is used as a background.

Breakthrough curves are established during toluene adsorption and desorption steps. Under dry air and 100 ppm toluene gas phase concentration, 3.4 ± 0.3 µmol/m$^2$ toluene are initially adsorbed on $CeO_2$. The flushing of toluene saturated $CeO_2$ surface by air leads to the desorption of 2.0 ± 0.2 µmol/m$^2$ of toluene subsequently considered as reversibly adsorbed. The amount of irreversibly adsorbed toluene on $CeO_2$ is given by the subtraction of these two values, i.e. 1.4 ± 0.2 µmol/m$^2$.

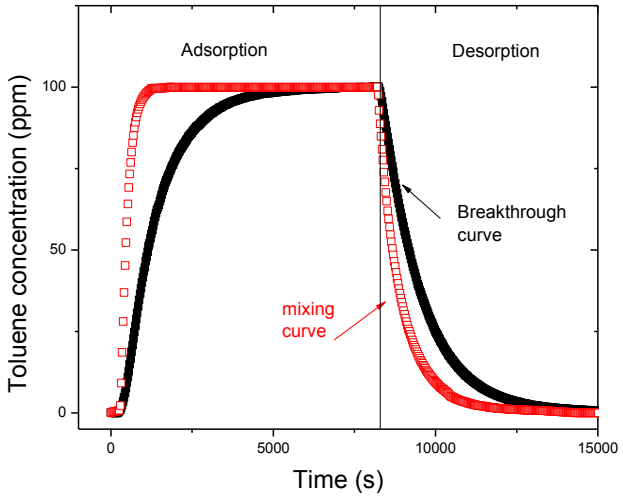


**Figure 5 - Breakthrough curve obtained during adsorption and desorption steps of the experimental procedure and used to quantify adsorbed toluene.**

Adsorbed phase measurements are monitored by DRIFTS. The Corresponding recorded spectra as a function of time are reported in Figure 6a and the evolution of toluene adsorption capacity is plotted in Figure 6b. The bands assignment was presented in section 2.2. During the toluene adsorption, the intensity of the bands increases as function of adsorption time. No other bands than that attributed to toluene were observed along toluene adsorption using DRIFTS and FTIR. It's shown in this section that since the spectra of adsorbed toluene on ceria could be recorded *in-situ,* the catalyst working can be monitored to investigate the changes of species during the adsorption and plasmas-oxidation. Besides, quantitative analysis of the gases leaving the DRIFTS cell provides additional data: toluene adsorption

capacity and by-products formation. A direct quantitative technique to investigate the adsorbed species on catalyst surface by transmission IR using ST is presented in next section.

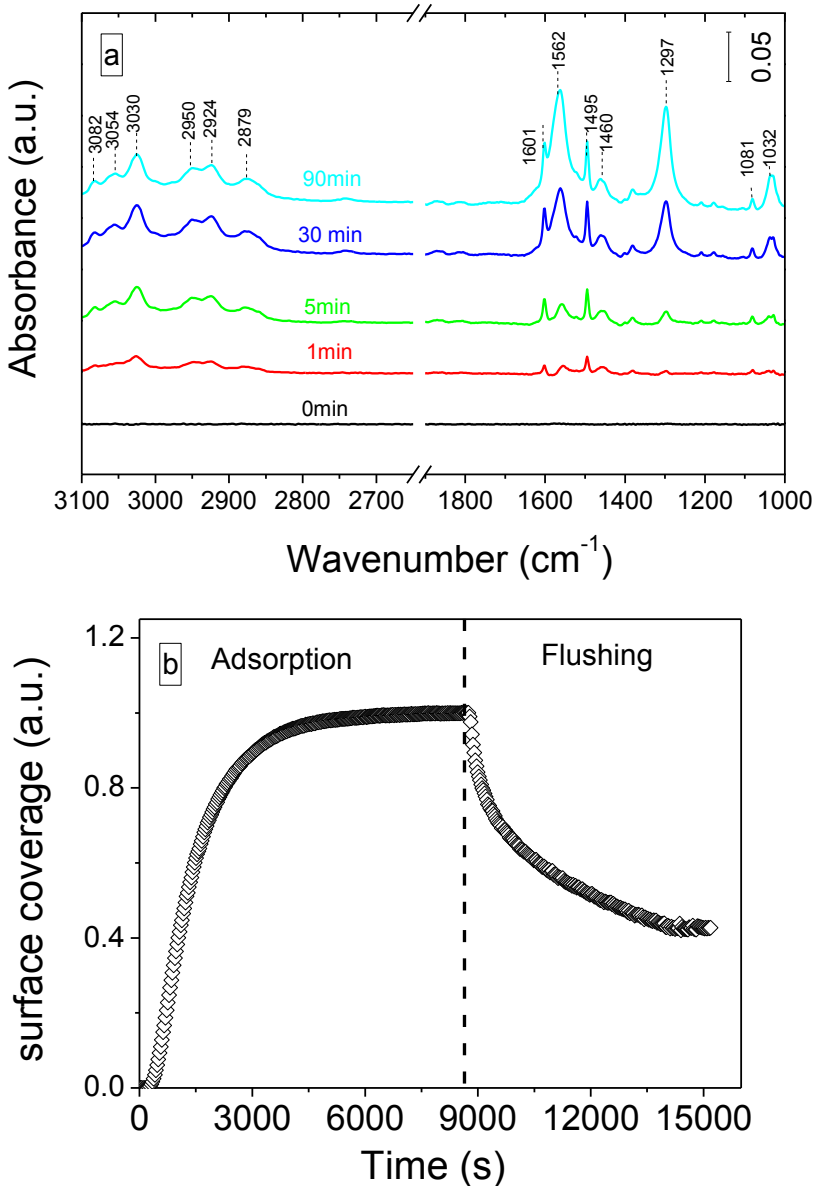


**Figure 6 - a) Absorbance spectra recorded by DRIFTS during toluene adsorption on $CeO_2$. (100 ppm toluene, 500 mL/min air, 25 mg $CeO_2$); b) the evolution of the adsorption and desorption by air of toluene on $CeO_2$.**

***In-Plasma (IPC) set-up***

For the IPC set-up, the same experiment condition as PPC is used to saturate the ceria surface by toluene. When using Sorbent Track, the quantitative method was presented in

section 2.3. In Sorbent-TRACK, toluene molecules may be located on the catalyst and in the gas phase. Hence the absorbance is:

$$A_{toluene} = 2.7x10^5 (\sigma^S_{toluene} + \sigma^G_{toluene}) \quad \textbf{Equation 4}$$

$\sigma^S_{toluene} + \sigma^G_{toluene}$ are the optical depth of toluene in the solid and gas phase respectively. In order to evaluate the contribution of the toluene gas phase molecules to the absorbance in ST cell, the infrared spectra of the $CeO_2$ surface upon toluene adsorption is recorded in Figure 7a and the evolution of toluene adsorption capacity is plotted in Figure 7b. With the gas flow of 500ml/min and the volume of ST cell of 460ml, the filling time is about 1 min. So the spectrum recorded at 1 min in Figure 7a by ST is mainly toluene of gas phase. The gas phase contribution of toluene is about 2% of toluene concentration at 90min. In the following (Figure 7b), the concentration of adsorbed toluene has been corrected from the gas phase contribution. Direct FTIR absorption is performed through the ceria sample. The total, reversible and irreversible amount of toluene is respectively determined as 2.9 ± 0.3, 1.6 ± 0.2, and 1.1 ± 0.2 µmol/m$^2$. These values are not significantly different from those obtained in PPC set-up, which confirms the performance of IPC set-up.

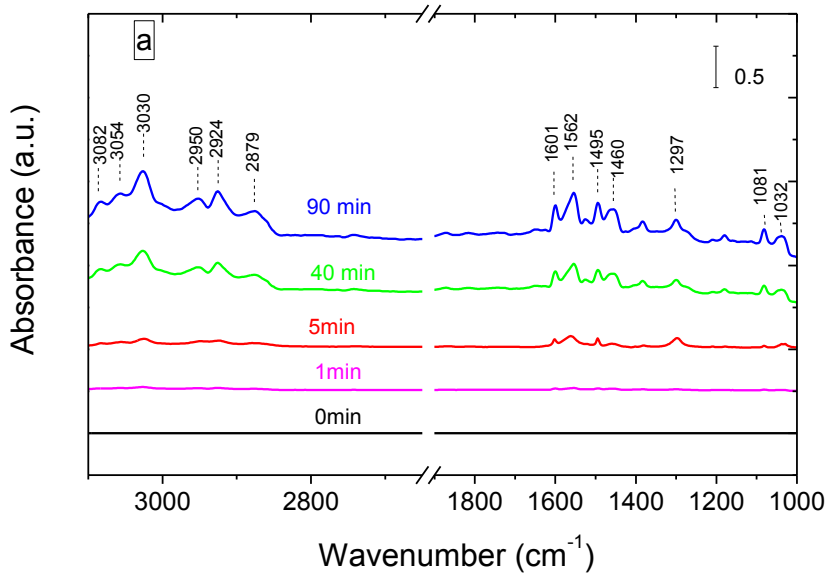

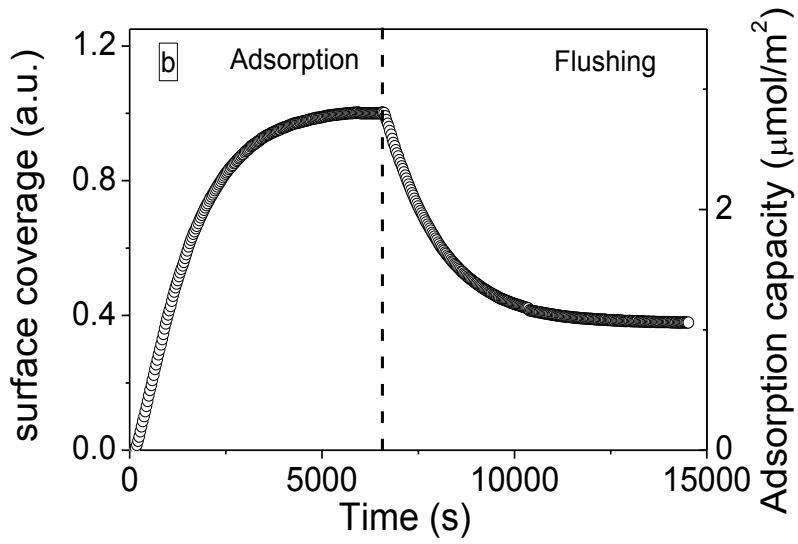


**Figure 7 a) Absorbance spectra recorded by Trans-FTIR in Sorbent Track during toluene adsorption on $CeO_2$. (100 ppm toluene, 500 mL/min air, 25 mg $CeO_2$); b) the evolution of the adsorption and desorption by air of toluene on $CeO_2$.**

## *3.2 Comparison of toluene oxidation in IPC and PPC*

Beyond toluene adsorption, which was quantitatively and qualitatively addressed in PPC and IPC configurations of by DRIFTS and ST, toluene oxidation is investigated using these two configurations. Figure 8a shows the temporal evolution of $CeO_2$ surface coverage by toluene under plasma exposure in IPC and PPC configurations for different plasma input powers. Two main comments can be made: i) an increase of the plasma power leads to an increase of oxidation rate; ii) higher toluene oxidation rate is achieved when there is direct contact between the plasma and cerium oxide surface (IPC). It was checked using a 10 long path cell FTIR absorption spectroscopy that no toluene is detected in the gas phase (sensitivity = 100 ppb), thus toluene desoprtion in PPC or IPC is excluded here. Meanwhile, the graph of Figure 8a represents concentration of reactants versus time considering a first-order reaction and the reaction rates corresponding input powers have been plotted in Figure 8b. Compared with PPC, the rate constants become higher in IPC. Regardless of the plasma configurations, rate constants are higher with more injected power and linearly increase with power. The

slopes η which are respectively $14x10^{-3}$ $J^{-1}$ and $7.6x10^{-3}$ $J^{-1}$ for IPC and PPC are not much sensitive to the injected power. The η of IPC is almost twice than PPC that higher toluene removal could be achieved with ceria in IPC than PPC under the same injected power.

Higher toluene removal in IPC can be also confirmed by literature. For PPC, ozone is the most important oxidizing agent from the following reaction:

$$\text{Toluene} + O_3 \rightarrow \text{Products } (k=1.2x10^{-20} cm^3/mol^{-1}s^{-1}) \text{ [30]} \qquad \text{Reaction 1}$$

$O_3$ can be catalytically decomposed into highly active atomic oxygen which is highly active and involved in toluene oxidation:

$$\text{Toluene} + O\cdot \rightarrow \text{Products } (k=2.32x10^{-13} cm^3/mol^{-1}s^{-1}) \text{ [31]} \qquad \text{Reaction 2}$$

Atomic oxygen can also react with water to form hydroxyl radical which is very powerful oxidants that enhance toluene destruction:

$$\text{Toluene} + OH\bullet \rightarrow \text{Products } (k=5.7x10^{-12} cm^3/mol^{-1}s^{-1}) \text{ [32]} \qquad \text{Reaction 3}$$

As for the IPC, short-life active species should be considered from the following reactions:

$$\text{Toluene} + e^- \rightarrow \text{Products } (k= 1\times10^{-6} cm^3/mol^{-1}s^{-1}) \text{ [33]} \qquad \text{Reaction 4}$$

$$\text{Toluene} + O^+, O_2^+, N^+ \text{ or } N_2^+ \rightarrow \text{Products } (k= 1\times10^{-10} cm^3/mol^{-1}s^{-1}) \text{ [34]} \qquad \text{Reaction 5}$$

Much more O• and OH• radicals can be formed in the IPC, which combines both gas-phase and catalyst surface. Besides of energetic electrons impact, radical attack is another important mechanism with a higher rate constants leading to toluene destruction in the IPC. These could explain that IPC is more effective for toluene removal with ceria than PPC.

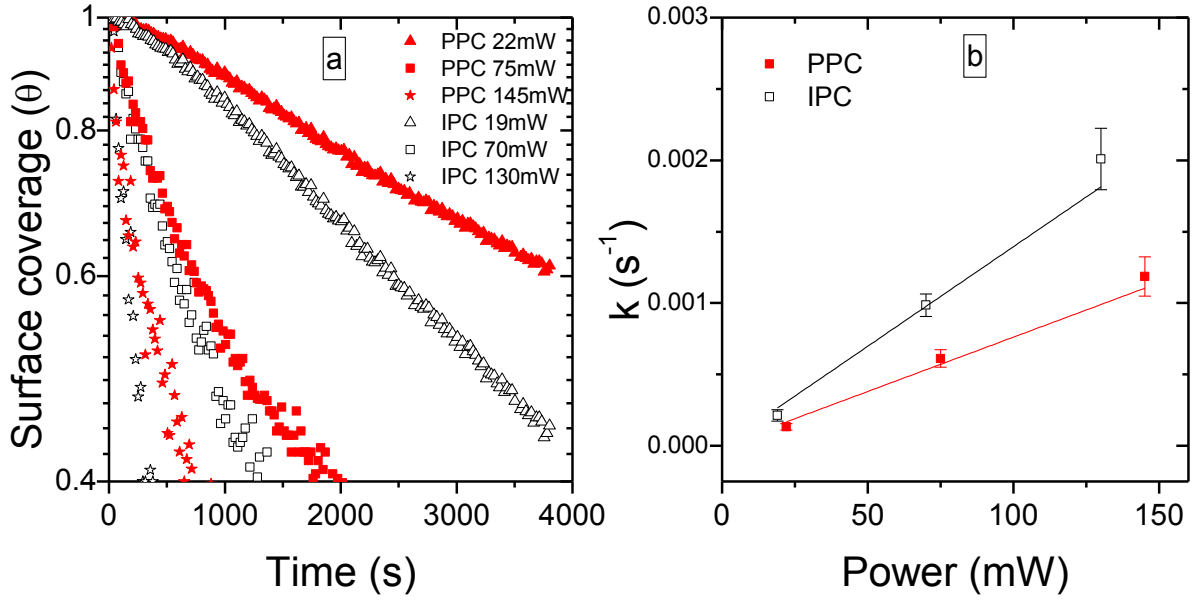


**Figure 8 - a) Evolution of toluene coverage on $CeO_2$ during NTP exposure at different injected powers which are respectively 22, 75 and 145 mW for PPC (red) and 19, 70 and 130 mW for IPC (black) (when ceria surface is saturated (θ=1), the adsorbed toluene value is 2.95 µmol for 25mg catalysts) and b) the rate constant obtained from Figure 8a at different injected powers for PPC (red) and IPC (black).**

## *3.3 Adsorbed intermediates study during toluene oxidation*

### *3.3.1 Adsorbed intermediates formation using PPC*

When the plasma is turned on, the catalytic surface is exposed to a flow of long-life reactive species - mainly ozone; C–H toluene aromatic bands (at around 3100–3000 $cm^{-1}$ domain) rapidly decrease during the first minute of plasma treatment, as shown in Figure 9. Some potential by-products were presented in section 2.3 which are used for the following discussions. The new bands at 2848, 1715, 1653, 1584, 1448, 1312 $cm^{-1}$ increase with time and can be attributed to adsorbed benzaldehyde [35]. The bands at 2848 and 1715 $cm^{-1}$ could be attributed to C-H and C=O of benzaldehyde. The bands at 1653, 1584 and 1312 $cm^{-1}$ arise from the different vibrational modes of aromatic rings. The presence of benzoic acid can be evidenced by 1754,1681, 1609, 1584, 1501,1448,1422, 1320 $cm^{-1}$ which are respectively assigned to ν(COOH), ν(CC)+δ(CH) ring (1609, 1584,1501, 1448 $cm^{-1}$ ) , δ(C-OH) and

vs(OCO) benzoate [36] . The δ(OH) at 1372 $cm^{-1}$ [36] and ν(CO) at 1016 and 1035 $cm^{-1}$ [37] ν(CC)+δ(CH) ring at 1609, 1584, 1501 [38] can be attributed to benzyl alcohol.

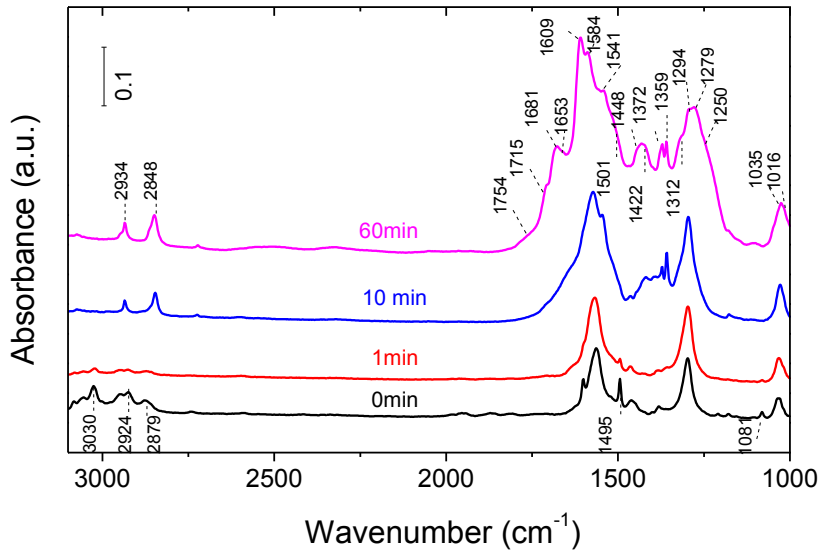


**Figure 9 - DRIFTS absorbance infrared spectra of surface species adsorbed on $CeO_2$ during post plasma treatment (500 mL/min air, 25 mg $CeO_2$, 294 K, 50 Hz, 15 kV, 145 mW, 60 min).**

Based on the integration of the bands at 2879 $cm^{-1}$, 1754 $cm^{-1}$, 1715 $cm^{-1}$ and 1016 $cm^{-1}$ respectively used for toluene, benzoic acid, benzaldehyde and benzyl alcohol surface semi-quantitative investigation, evidences the temporal profiles of toluene and its oxidation products. At t = 0 min corresponding to the end of flushing step and the beginning of plasma exposure, $CeO_2$surface is saturated with toluene under the corresponding gas phase concentration and $\theta_{Toluene}$ is considered as 1,i.e. 1.4 µmol adsorbed per $m^2$ or 118 µmol of toluene adsorbed per gram of $CeO_2$. Figure 10 shows a decrease in toluene surface coverage and the formation of adsorbed intermediates such as benzyl alcohol (1016 $cm^{-1}$), benzaldehyde (1715 $cm^{-1}$) and benzoic acid (1754 $cm^{-1}$) as soon as the plasma is turned on. Simultaneously a production of adsorbed benzyl alcohol and benzaldehyde is observed. Their surface concentrations gradually increase until plateau is reached, i.e. ca. 2000s and 3000s respectively after *post-situ* plasma exposure. The evolution of benzoic acid differs from that

of benzyl alcohol and benzaldehyde. Indeed, the production of surface benzoic acid starts beyond 500s while no benzoic acid is observed in the gas phase.

As mentioned in section 3.2, in PCC ozone is the most important oxidizing agent and it can be catalytically decomposed into highly active atomic oxygen which reacts with water to form hydroxyl radical. The atomic oxygen and hydroxyl radical play an important role during toluene oxidation [33,39–42]. The hydrogen abstraction from the methyl group is the primary pathway in toluene oxidation, leading to a benzyl radical and then forming benzaldehyde and benzyl alcohol, which will be further attacked by an atomic oxygen and hydroxyl radical forming benzoic acid [42]. Toluene and these three initial by-products (benzaldehyde, benzyl alcohol and benzoic acid) were attacked by atomic oxygen and hydroxyl radical addition to the aromatic ring, which resulted in the open of aromatic ring [40]. The compounds generated after ring opening contained several carbonyl bonds (C=O) and alkenyl bonds (C=C), finally leading to the formation of harmless $CO_2$ and $H_2O$.

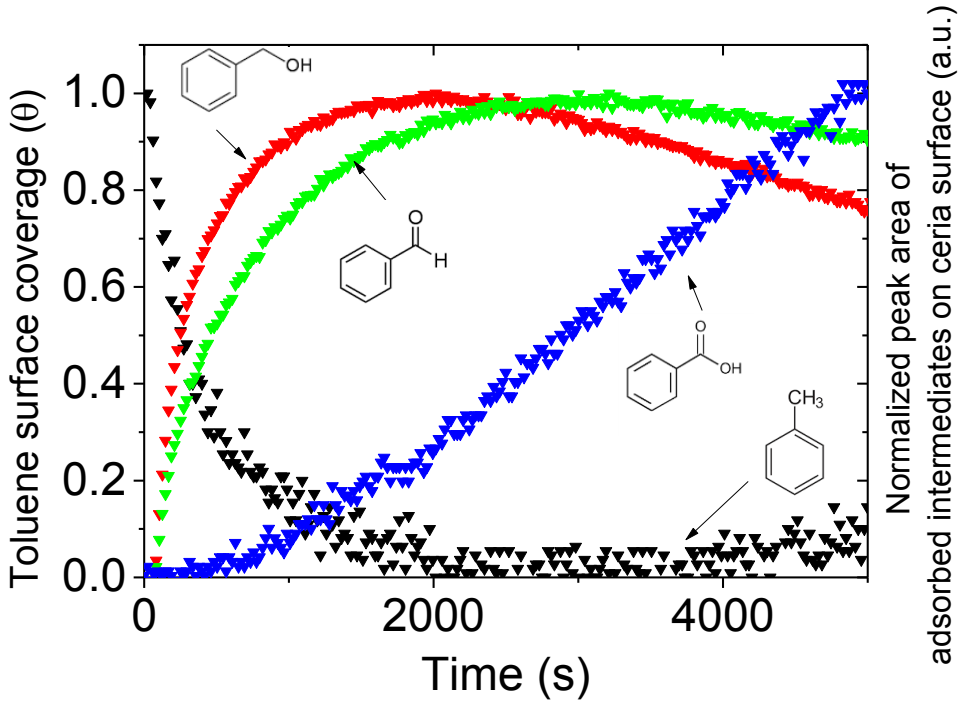

**Figure 10 - Evolution of toluene surface coverage on $CeO_2$ as a function of post-situ NTP exposure time. Adsorbed intermediates such as benzyl alcohol (1016 $cm^{-1}$), benzaldehyde (1715 $cm^{-1}$) and benzoic acid (1754 $cm^{-1}$) are also plotted.**

### *3.3.2 Adsorbed intermediates formation using IPC*

In the case of the *in-plasma* Configuration, the catalytic surface is simultaneously exposed to short and long life species produced by the plasma. Figure 11, shows the dynamic of spectra recorded by Sorbent-TRACK after the plasma has been turned ON while the evolution of toluene and adsorbed intermediates are plotted in Figure 12. Compared to the PPC configuration, some similar trends have been observed: 1) the C–H aromatic bands (at around 3100–3000 $cm^{-1}$ domain) decreased rapidly at the first minutes of plasma treatment; 2) the presence of benzyl alcohol (1016 $cm^{-1}$), benzaldehyde (1715 $cm^{-1}$) and benzoic acid (1754$cm^{-1}$) have been confirmed by the bands discussed in the previous section. However, the bands in the region of 1600-1700 $cm^{-1}$, which correspond benzaldehyde are less intense in IPC configuration than in PPC configuration. Moreover, ring opening reactions could be supported by the presence of C=O at a band between 1770-1740 $cm^{-1}$ which may correspond the carbonyl group [43] and by the increasing and broadening of the 1400-1500 $cm^{-1}$ band which could be due to various stretching behaviors such as C=C from alkenes [44]. The presence of alkane groups is indicated by the C-H bending vibration between 1380 and 1465 $cm^{-1}$ and the location of bending vibration of $CH_3$ groups at 1390 $cm^{-1}$ could be given as evidence. The bands at 1582, 1520 and 1290 $cm^{-1}$ could be assigned according to literature [45–47] to surface nitrates species, like nitrobenzene.

The mechanism of toluene oxidation in IPC is more complex than PPC because in IPC toluene could react with short live species, especially electron. The contribution of electron is not negligible as the reaction rate constant (in reaction 4) is important. The authors [33,39,48] propose that the toluene destruction is mainly initiated via the collision between an electron in plasma and toluene molecules with the formation of phenyl radical and methyl. Mean energy

of C–C between the methyl group and the aromatic ring is about 4.4 eV [34] while mean energy of the energetic electrons ranges from 1 to 10 eV [49] that C–C can be easily destructed by energetic electrons beyond 4.4 eV. Phenyl radical could react with excited $NO_2$• , forming nitrobenzene. The radical attack (atomic oxygen and hydroxyl radical) would occur subsequently and contribute to toluene oxidation and ring opening reactions. Toluene destruction consists of several processes in IPC, and its destruction by energetic electrons and radicals are inseparable and cooperative which make IPC is more effective than PPC for toluene removal.

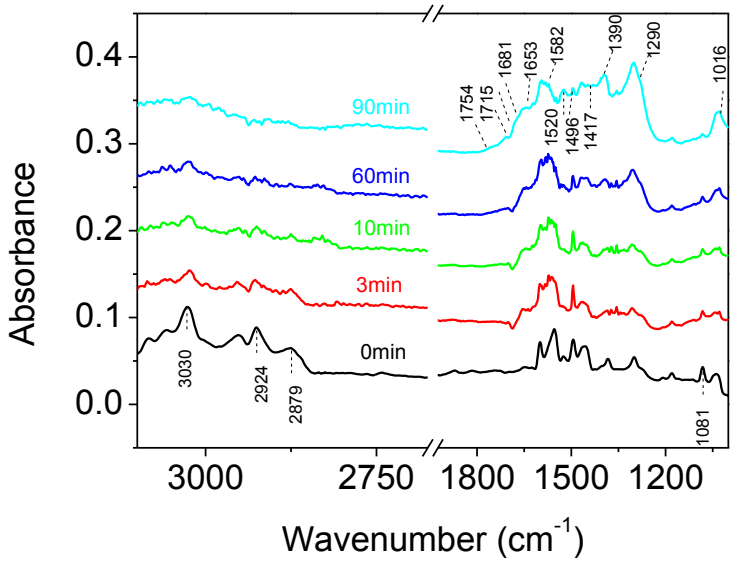


**Figure 11 - Transmission infrared absorbance spectra of surface species adsorbed on $CeO_2$ during post plasma treatment using Sorbent Track (500 mL/min air, 15 mg $CeO_2$, 294 K, 50 Hz, 10 kV, 70mW, 90 min).**

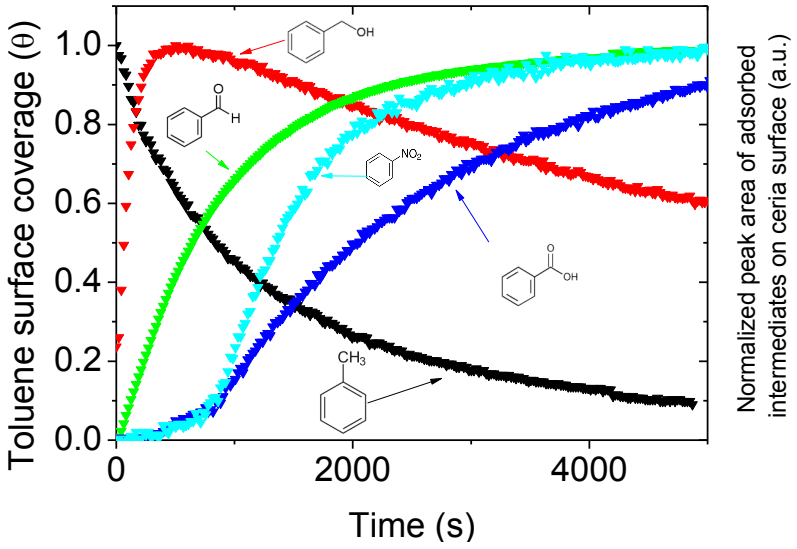


**Figure 12 - Evolution of toluene surface coverage on $CeO_2$ as a function of *in-situ* NTP exposure time. Adsorbed intermediates such as benzyl alcohol (1016 $cm^{-1}$), benzaldehyde (1715 $cm^{-1}$), benzoic acid (1754 $cm^{-1}$) and nitrobenzene (1520 $cm^{-1}$) are also plotted.**

# 4 Conclusion

In this study, we present the dynamic *in-situ* monitoring of the adsorption followed by the oxidation of toluene adsorbed on Ceria under plasma exposure in two different plasma configurations: In-Plasma and Post-Plasma Configurations where the catalyst is located in contact with the plasma or downstream the plasma.

Diffuse Reflectance Infrared Fourier Transform Spectroscopy (DRIFTS) and Trans-FTIR have been respectively used to monitor the ceria surface in the post-situ plasma (PPC) and *in-situ* plasma (IPC) configuration. A new dedicated device, Sorbent-TRACK has been set-up to perform Trans-FTIR experiments in IPC configuration. The adsorption of toluene on ceria was quantitatively and qualitatively analyzed in the configuration of PPC and IPC by DRIFTS and ST respectively and the adsorption capacity is respectively 1.4 ± 0.2 and 1.1 ± 0.2 µmol/$m^2$. It was found that the toluene oxidation by plasma is a first-order reaction and IPC is more effective for the toluene removal than PPC. Regardless of the plasma configurations,

rate constants increase linearly with injected power. The adsorbed intermediates were also monitored by DRIFTS and transmission IR. The long live species and short live species lead to different intermediates formation and evolution which could explain the higher efficiency of toluene removal in IPC.

## *Acknowledgements*

This work has been done within the French DGA project of 2012 60 013 00470 7501, and the LABEX PLAS@PAR project by the Agence Nationale de la Recherche under the reference ANR-11-IDEX-0004-02.

# *References*


[1] J. L. Domingo, M. Nadal, *Environ. Int.* **2009**, *35*, 382.

[2] S. C. Lee, M. Y. Chiu, K. F. Ho, S. C. Zou, X. Wang, *Chemosphere* **2002**, *48*, 375.

[3] P. Grandjean, P. Landrigan, *Lancet* **2006**, *368*, 2167.

[4] V. Augugliaro, S. Coluccia, V. Loddo, L. Marchese, G. Martra, L. Palmisano, M. Schiavello, *Appl. Catal. B Environ.* **1999**, *20*, 15.

[5] M. A. Lillo-Ródenas, D. Cazorla-Amorós, A. Linares-Solano, *Carbon N. Y.* **2005**, *43*, 1758.

[6] A. B. Darlington, J. F. Dat, M. A. Dixon, *Environ. Sci. Technol.* **2001**, *35*, 240.

[7] J. Van Durme, J. Dewulf, W. Sysmans, C. Leys, H. Van Langenhove, *Appl. Catal. B Environ.* **2007**, *74*, 161.

[8] H.-H. Kim, *Plasma Process. Polym.* **2004**, *1*, 91.

[9] F. Thevenet, L. Sivachandiran, O. Guaitella, C. Barakat, A. Rousseau, *J. Phys. D. Appl. Phys.* **2014**, *47*, 224011.

[10] Z. Jia, A. Vega-Gonzalez, M. Ben Amar, K. Hassouni, S. Tieng, S. Touchard, A. Kanaev, X. Duten, *Catal. Today* **2013**, *208*, 82.

[11] X. Zhu, X. Gao, X. Yu, C. Zheng, X. Tu, *Catal. Today* **2015**, *256*, 108.

[12] X. Zhu, S. Liu, Y. Cai, X. Gao, J. Zhou, C. Zheng, X. Tu, *Appl. Catal. B Environ.* **2016**, *183*, 124.

[13] S. Sauce, A. Vega-González, Z. Jia, S. Touchard, K. Hassouni, A. Kanaev, X. Duten, X. Duten, *Eur. Phys. J. Appl. Phys.* **2015**, *71*, 20805.

[14] M. A. Malik, Y. Minamitani, K. H. Schoenbach, *IEEE Trans. Plasma Sci.* **2005**, *33*, 50.

[15] U. Roland, F. Holzer, F.-D. Kopinke, *Appl. Catal. B Environ.* **2005**, *58*, 217.

[16] A. Ogata, K. Saito, H.-H. Kim, M. Sugasawa, H. Aritani, H. Einaga, *Plasma Chem. Plasma Process.* **2010**, *30*, 33.

[17] J. Van Durme, J. Dewulf, K. Demeestere, C. Leys, H. Van Langenhove, *Appl. Catal. B Environ.* **2009**, *87*, 78.

[18] J. Woloszko, K. R. Stalder, I. G. Brown, *IEEE Trans. Plasma Sci.* **2002**, *30*, 1376.

[19] H.-H. Kim, A. Ogata, S. Futamura, *Appl. Catal. B Environ.* **2008**, *79*, 356.

[20] L. Chen, J. Li, M. Ge, *Environ. Sci. Technol.* **2010**, *44*, 9590.

[21] A. Aguirre, C. E. Barrios, A. Aguilar-Tapia, R. Zanella, M. A. Baltanás, S. E. Collins, *Top. Catal.* **2016**, *59*, 347.

[22] S. H. Pang, C. A. Schoenbaum, D. K. Schwartz, J. W. Medlin, *Nat. Commun.* **2013**, *4*, 2448.

[23] S. Sauce, A. Vega-González, Z. Jia, S. Touchard, K. Hassouni, A. Kanaev, X. Duten, *Eur. Phys. J. Appl. Phys.* **2015**, *71*, 20805.

[24] C. Barakat, P. Gravejat, O. Guaitella, F. Thevenet, A. Rousseau, *Appl. Catal. B Environ.* **2014**, *147*, 302.

[25] M. Magureanu, D. Piroi, N. B. Mandache, V. I. Pârvulescu, V. Pârvulescu, B. Cojocaru, C. Cadigan, R. Richards, H. Daly, C. Hardacre, *Appl. Catal. B Environ.* **2011**, *104*, 84.

[26] M. Rivallan, E. Fourré, S. Aiello, J.-M. Tatibouët, F. Thibault-Starzyk, *Plasma Process. Polym.* **2012**, *9*, 850.

[27] C. E. Stere, W. Adress, R. Burch, S. Chansai, A. Goguet, W. G. Graham, C. Hardacre, *ACS Catal.* **2015**, *5*, 956.

[28] Z. Jia, A. Rousseau, *Sci. Rep.* **2016**, *6*, 31888.

[29] G. BUSCA, F. Cavani, F. Trifirò, *J. Catal.* **1987**, *106*, 471.

[30] D. H. Stedman, H. Niki, *Environ. Lett.* **1973**, *4*, 303.

[31] J. T. Herron, R. E. Huie, *J. Phys. Chem. Ref. Data* **1973**, *2*, 467.

[32] B. Bohn, *J. Phys. Chem. A* **2001**, *105*, 6092.

[33] H. Huang, D. Ye, D. Y. C. Leung, F. Feng, X. Guan, *J. Mol. Catal. A Chem.* **2011**, *336*, 87.

[34] H. Kohno, A. A. Berezin, Jen-Shih Chang, M. Tamura, T. Yamamoto, A. Shibuya, S. Honda, *IEEE Trans. Ind. Appl.* **1998**, *34*, 953.

[35] L. Cao, Z. Gao, S. L. Suib, T. N. Obee, S. O. Hay, J. D. Freihaut, *J. Catal.* **2000**, *196*, 253.

[36] C. Keresszegi, D. Ferri, T. Mallat, A. Baiker, *J. Phys. Chem. B* **2005**, *109*, 958.

[37] E. Nowicka, J. P. Hofmann, S. F. Parker, M. Sankar, G. M. Lari, S. A. Kondrat, D. W. Knight, D. Bethell, B. M. Weckhuysen, G. J. Hutchings, *Phys. Chem. Chem. Phys.* **2013**, *15*, 12147.

[38] R. Méndez-Román, N. Cardona-Martínez, *Catal. Today* **1998**, *40*, 353.

[39] J. Van Durme, J. Dewulf, W. Sysmans, C. Leys, H. Van Langenhove, *Chemosphere* **2007**, *68*, 1821.

[40] T. J. Frankcombe, S. C. Smith, *J. Phys. Chem. A* **2007**, *111*, 3686.

[41] T. J. Frankcombe, S. C. Smith, *J. Phys. Chem. A* **2007**, *111*, 3691.

[42] J. Mo, Y. Zhang, Q. Xu, Y. Zhu, J. J. Lamson, R. Zhao, *Appl. Catal. B Environ.* **2009**, *89*, 570.

[43] A. Rodrigues, J.-M. Tatibouët, E. Fourré, *Plasma Chem. Plasma Process.* **2016**, *36*, 901.

[44] F. Rainone, D. A. Bulushev, L. Kiwi-Minsker, A. Renken, *Phys. Chem. Chem. Phys.* **2003**, *5*, 4445.

[45] T. Chafik, S. Kameoka, Y. Ukisu, T. Miyadera, *J. Mol. Catal. A Chem.* **1998**, *136*, 203.

[46] K. Hadjiivanov, D. Klissurski, G. Ramis, G. Busca, *Appl. Catal. B Environ.* **1996**, *7*, 251.

[47] A. Łamacz, A. Krztoń, G. Djéga-Mariadassou, **n.d.**

[48] W. J. Liang, L. Ma, H. Liu, J. Li, *Chemosphere* **2013**, *92*, 1390.

[49] Y.-F. Guo, D.-Q. Ye, K.-F. Chen, J.-C. He, W.-L. Chen, *J. Mol. Catal. A Chem.* **2006**, *245*, 93.

Table of Contents

Toluene adsorption and oxidation on $CeO_2$ surface by Non-thermal plasma (NTP) is *in-situ* monitored using infrared (IR) diagnostics (Diffuse Reflectance Infrared Fourier Transform Spectroscopy (DRIFTS) and transmission mode). The oxidation of toluene by plasma follows a first-order reaction regardless of plasma configuration and injected power. It was found that IPC was more effective for the toluene removal than PPC. Interestingly, toluene abatement and reaction intermediate formations are characterized *in-situ* throughout the heterogeneous oxidation reaction advancement.